Quantitative assessment and spatial distribution of *Plasmopara viticola* oospores in vineyard soil

Charlotte Poeydebat[1], Eva Courchinoux[2], Isabelle Demeaux[2], Marie Rodriguez[2], Alexandre Chataigner[2], Mélanie Lelièvre[3], Jean-Pascal Goutouly[4], Jean-Pierre Rossi[5], Marc Raynal[6], Laurent Delière[2], François Delmotte[2]

Affiliations

[1] Bordeaux Sciences Agro, INRAE, SAVE, ISVV, 33175 Gradignan, France

[2] INRAE, Bordeaux Sciences Agro, SAVE, ISVV, 33882 Villenave d'Ornon, France

[3] Université Bourgogne Franche-Comté, INRAE, AgroSup Dijon, Agroécologie, 21000 Dijon, France

[4] INRAE, Université de Bordeaux, Bordeaux Sciences Agro, UMR EGFV, ISVV, 33882 Villenave d'Ornon, France

[5] INRAE, CIRAD, IRD, Institut Agro, CBGP, 34988 Montferrier-sur-Lez, France

[6] IFV, Bordeaux Nouvelle Aquitaine, UMT SEVEN, 33882 Villenave d'Ornon Cedex, France

Corresponding author: Charlotte Poeydebat, charlotte.poeydebat@agro-bordeaux.fr

Abstract

Grapevine downy mildew, caused by the oomycete *Plasmopara viticola*, is one of the most devastating diseases of grapevine worldwide. While primary inoculum plays a decisive role in disease epidemics, we still know very little about the abundance and the distribution of oospores, which are the overwintering forms of the pathogen resulting from sexual reproduction. In this study, we used ddPCR to describe the

spatial distribution of *P. viticola* inoculum in a vineyard soil at the onset of the growing season. We found *P. viticola* oospores in all soil samples except one. The distribution of primary inoculum at the field scale was not random but characterized by 25 m-diameter patches of concentrically increasing oospore concentration. There was a positive coregionalization between soil inoculum and soil moisture spatial distributions, possibly mediated by disease incidence. The results indicated that oospores accumulated 5 times more in the ridge of soil below the vine stocks than in the inter-row. We conducted a leaf disc bioassay to assess soil infectious potential on a subset of samples collected in the field. Soil infectious potential estimated through infected leaf-disc area was positively correlated with our DNA-based quantification of oospores. Overall, the quantitative and spatially explicit survey of primary inoculum reservoir gained from these molecular and biological methods will contribute to the design of management strategies aimed at preventing primary inoculum accumulation in the vineyard from one season to the next.

Keywords: oomycete, downy mildew, *sexual reproduction,* primary inoculum, geostatistics, ddPCR, bioassay, soil infectious potential

Introduction

Grapevine downy mildew, caused by the obligate biotrophic oomycete *Plasmopara viticola*, is one of the most devastating diseases of grapevine worldwide. Its management still relies mainly on intensive use of fungicides throughout the growing season, which leads to environmental pollution threatening both biodiversity (Beaumelle et al. 2023; Beketov et al. 2013) and human health (e.g. Dall'Agnol et al., 2021). Moreover, the efficacy of this fungicide-based strategy may decrease over time due to the emergence of pathogen resistant strains (Chen et al. 2007; Delmas

et al. 2017). As large spectrum multisite fungicides are increasingly banned in Europe, the substitutive use of unisite products will increase the risk for resistance apparition because fewer mutations in the pathogen genome will be necessary. In France, recent public policies have clearly encouraged the reduction of the use of chemical plant protection products (National Action Plan Ecophyto; Lamichhane et al., 2019). Accordingly, major efforts are currently underway to develop alternative methods to manage grapevine downy mildew epidemics, including genetically resistant grapevine varieties and biosolutions (e.g., biocontrol or biostimulation products). Some studies have shown that the efficacy of biocontrol products or agents may be limited (e.g., only 36.5% of substance/dosage combinations were as effective as the copper standard in Dagostin et al., 2011) or even unsatisfactory in real conditions due to their sensitivity to environmental factors (e.g., rain, UV radiation; Dagostin et al., 2011). On the other hand, the development of grapevine resistant varieties is a long process, their adoption is slowed down by AOP regulation on authorized varieties, and resistance durability may be limited in time due to resistance breakdown by pathogens (Peressotti et al. 2010). All of these methods are curative and/or affect the pathogen during its asexual cycle and the grapevine growing season. In addition, there is a need to develop preventive methods that lower the epidemic risk at the source.

In temperate regions, the life cycle of *P. viticola* alternates between asexual multiplication on its host tissues during the growing season and obligatory sexual reproduction, which allows for overwintering in the soil compartment. Sexual reproduction occurs in infected grapevine leaves between thalli of sexually compatible strains (as *P. viticola* is heterothallic, Wong et al., 2001) leading to the formation of oospores. Leaves then fall on the ground, and oospores overwinter in

leaf debris or as free propagules in the soil. The stock of oospores in the soil constitutes the primary inoculum for downy mildew epidemics in the next growing season. In contrast to the widely-held assumption that primary contaminations rarely occur after flowering, primary inoculum is increasingly considered to play a major role in grapevine downy mildew epidemics (Gessler et al. 2011) for several reasons. First, population genetic studies evidenced that grapevine downy mildew populations are panmictic across european vineyards (Fontaine et al. 2021, 2013) showing that genetic mixing resulting from sexual reproduction largely structures pathogen populations. Second, it has been shown that oospores are able to germinate and cause infections throughout the growing season (until late September in the northern hemisphere; Kennelly et al., 2007; Maddalena et al., 2021) and that a substantial amount of infections, including in the middle of the growing season, can arise from sexually derived inoculum (oospores) on a field scale (up to 50% of contaminations; Gobbin et al., 2003; Hong et al., 2020). Third, as the epidemic continues to progress after harvest, the incidence of typical mosaic-like downy mildew symptoms on grapevine leaves was shown to be proportional to the amount of oospores formed in the leaves (Maddalena et al. 2021). Finally, downy mildew incidence at the end of the season was found to explain the precocity and intensity of the disease the following season in a Canadian vineyard (Carisse 2016).

The notable contribution of *P. viticola* primary inoculum to epidemic dynamics suggests that prophylactic measures based on primary inoculum management or interruption of the pathogen's life cycle from one season to the next have the potential to significantly reduce epidemic pressure. Prophylactic measures are often used in annual crops, involving mostly cultural practices such as mechanical destruction or removal of crop residues containing disease inoculum, but rarely in

perennial crops. However, a study of prophylactic disease management in apple orchards showed that the sweeping and plowing of apple leaf litter affected by apple scab resulted in significant reduction of the primary inoculum (*i.e. Venturia inaequalis* ascospores released from pseudothecia) and disease severity the next year (Gomez et al. 2007). We believe that limiting inter-annual inoculum accumulation could be particularly relevant for disease management in perennial cropping systems, such as vineyards, where crop rotation is impossible and pathogens are well established, more importantly if pesticides are being phased out.

Understanding the drivers of spatio-temporal variations in primary inoculum abundance is key to identifying levers for the preventive management of epidemic risk. At the leaf level, disease severity was found to be proportional to the amount of oospores formed per unit of leaf biomass (Maddalena et al. 2021). At the field scale, we hypothesized that the spatial variation in foliage disease severity explains the spatial variation in the abundance of primary inoculum because leaves (the oospore reservoir) remain close to the vine stock they fell from (*i.e.* a local accumulation of primary inoculum). Consequently, any spatially variable factor influencing downy mildew incidence over the course of the growing season could indirectly influence the distribution of primary inoculum in the soil. This effect should be stronger for factors that vary little with time (between years), as soil primary inoculum is the result of pluriannual accumulation of oospores that survive several years (Caffi et al. 2011). As an oomycete, *Plasmopara viticola* is particularly dependent on humidity at all stages of its life cycle (Gessler et al. 2011). For instance, soil moisture is required to trigger oospore germination and primary contaminations (Vercesi et al. 2010), while a longer leaf wetness duration promotes leaf infections by downy mildew. Excessive grapevine vigor (defined as a propensity to assimilate, store, and/or use

nonstructural carbohydrates for producing large canopies, associated with intense metabolism and fast shoot growth ; Hugalde et al., 2019) can result in increased susceptibility to disease, as high foliage density limits air movement and light penetration, as well as pesticide cover. In a study conducted in Germany, it was shown that canopy architecture (or foliage density) can affect canopy microclimate and *in fine* susceptibility to grapevine downy mildew. More precisely, minimally pruned Chardonnay grapevines with large-volume canopies (*i.e.* vigorous) exhibited increased leaf wetness, higher relative humidity, and greater rates of downy mildew infection, as compared to intensively pruned grapevines with less dense foliage (Pennington 2019). Hence, spatial variation in soil moisture and grapevine vigor, for instance, could induce spatial variation in disease severity, resulting in spatial variation in soil primary inoculum concentration.

Although the stages of the sexual reproduction cycle of *P. viticola* are well known (see for example Gessler et al., 2011), their quantitative description remains incomplete. DNA extraction methods and ITS-based molecular approaches have been developed and used to quantify airborne inoculum and oospores in leaves (Douillet et al. 2022; Si Ammour et al. 2020; Valsesia et al. 2005). To our knowledge, no methods have been adapted to survey *P. viticola* in the soil compartment. The assessment of downy mildew epidemic risk mainly relies on meteorological indicators that control the development of *P. viticola*. Direct indicators of the pathogen abundance in the vineyards, such as spore concentration in the air, are progressively included in decision tools or regional monitoring programs (Brischetto et al. 2020; Douillet 2023). However, indicators of primary inoculum reservoir in the soil compartment have never been used yet. They are not considered relevant predictors of epidemic risk, maybe because vineyard soils are implicitly considered

to be saturated with primary inoculum. The truth is that we have very little information on this point and on the relationship between the amount of inoculum and the risk of infection. Another key step in the development of preventive methods based on primary inoculum management will consist of evaluating the epidemiological significance of primary inoculum indicators.

Here, we present a new and repeatable method to assess downy mildew primary inoculum abundance in vineyard soil based on the quantification of *P. viticola* DNA by ddPCR. We used this method to provide quantitative and comprehensive insights on downy mildew sexual cycle epidemiology. By means of geostatistics, we described the spatial distribution of downy mildew primary inoculum in a vineyard at the onset of the growing season. Furthermore, we explored whether soil moisture or vine vigor spatial patterns could explain primary inoculum distribution, as mediated by disease severity and under the hypothesis of local accumulation of primary inoculum. If *P. viticola* oospores can persist in the soil and remain infectious for several years (Caffi et al. 2011), the determinants of oospore germination rate are poorly understood in natural conditions and the effect of aging of oospores on germination probability remains unstudied to date. However, we hypothesized that the DNA-based quantification of primary inoculum in the soil is positively related to grapevine primary contamination risk arising from the soil. Building on previous works (Hill 1998; Pertot and Zulini 2003), we finally present a bioassay to assess the infectious potential of soil samples and discuss the epidemiological significance of our DNA-based assessments of downy mildew primary inoculum. We believe that our work represents a significant step toward the design, evaluation and implementation of innovative and cost-effective disease monitoring methods and

preventive disease control strategies based on inter-annual primary inoculum management.

Material & Methods

Soil sampling and preparation

We conducted our study in an experimental vineyard with a sandy-gravel soil located at the INRAE Bordeaux Nouvelle-Aquitaine research center (Villenave d'Ornon, France; 44.79194, -0.57702) within the Pessac-Léognan appellation area. The surveyed vineyard was planted in 2011 with 18 rows of 68 Merlot grapevine stocks over a 0.22 ha surface (70 x 32 m), corresponding to a density of 6600 vines per ha (*i.e*. 1.6 m between rows and 0.95m between vines along the row). It was managed according to French organic farming specifications, meaning that Bordeaux mixture (copper) was the only chemical fungicide allowed to control downy mildew. Inter-rows were either sown with a mix of plant species selected for green manuring or covered by spontaneous vegetation in an alternating arrangement rotating every year. All inter-rows were tilled before grapevine budburst. For winter protection and weed management purposes, soil from both sides of the row was turned over on the lower part of the vines in the fall. The ridge formed under the row was then reopened in the spring. The surveyed vineyard was bordered on each of its long sides by a diversified shrubby hedgerow (*ca*. 1.5-2 m high) that separated it from other experimental vineyards.

Soil sampling was done in February 2022, the time of year when *P. viticola* DNA measurements are best related to the infectious potential for the upcoming growing season for several reasons: i) leaf decomposition and oospore incorporation into the

soil matrix are well advanced; ii) unviable oospores have degenerated; iii) the progressive oospore maturation process has run its course and the % of viable oospores is at its peak (Maddalena et al. 2021; Vercesi et al. 1999); and iv) oospore germination has not yet started (soil temperature still <11°C). We collected 198 soil samples at the nodes of a 2.85 x 3.2 m regular grid covering the entire surface of the vineyard; *i.e.* one sample every three vine stocks in the row, in one row out of two (Figure 1). To explore the spatial structure of primary inoculum of downy mildew in the soil at a finer scale within a feasible sampling framework, we delineated five plots in the experimental vineyard within which we collected soil samples following a nested sampling design with three distance levels. Each plot consisted of a 2.85 x 3.2 m rectangle containing 28 sampling points (Figure 1). The first distance level corresponded to the four corners of the plot (n_3=4), hence sampling points were separated by about 3 m (samples were the same as for the regular grid sampling). The second distance level was set at 0.8 m (half the inter-row width), and sampling points were located in the corners of four 0.8 m squares located in each corner of the plot ($n_{0.8}$=16, including 4 points in common with the first distance level; see figure 1). The third distance level was set at 0.2 m with sampling points corresponding to the corners of four 0.2 m squares located in the corners of one of the four 0.8 m squares ($n_{0.2}$=16, including 1 point in common with the first distance level and 4 points in common with the second distance level; see figure 1). We also considered that the points from the regular grid were located in the row, while the points from the 2nd and 3rd levels of the nested sampling were located in the inter-row space. At each sampling point of both the regular grid and the nested sampling plots, we collected 500 g of soil from the top 15 cm.

To investigate the vertical distribution of *P. viticola* primary inoculum in the soil, we dug a hole 40 cm deep and ca. 30 cm in diameter at six points located in the inter-row space in the experimental vineyard (Figure 1). We divided the soil profile into four strata of 10 cm (0-10, 10-20, 20-30 and 30-40 cm) and sampled 500 g of soil from each stratum, starting at the bottom of the profile to avoid contaminating deeper layers with upper ones. This corresponded to 24 samples in total. All soil samples were stored at 5°C before processing.

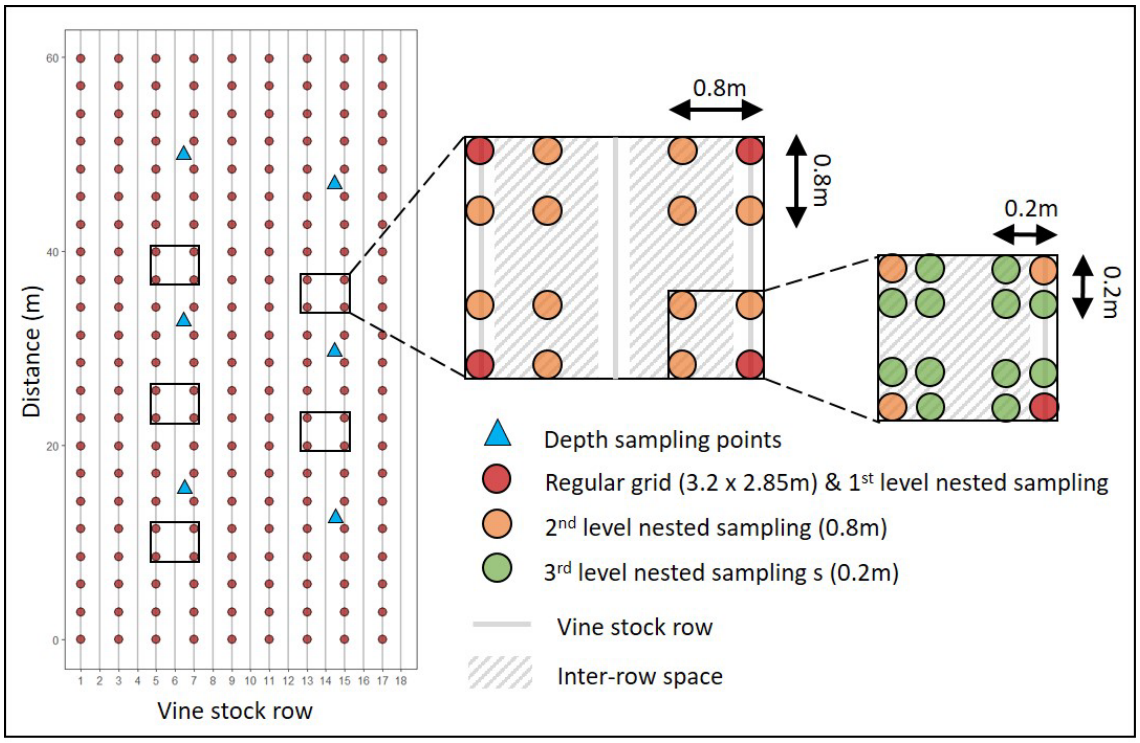

Figure 1. Map of the soil sampling points within the experimental vineyard.

Quantification of Pv primary inoculum in vineyard soil samples

DNA extraction

Each sample was passed through a 4 mm mesh sieve and thoroughly homogenized for 30 s using an electric mixer set at medium speed. Directly after homogenization, *ca*. 6 g of the sample was collected and placed in a 5 ml tube to be freeze-dried.

Then, a 2 g subsample of dry soil was placed in a 15 ml Falcon tube containing 4 g of 0.1 mm diameter silica beads, 5 g of 1.4 mm diameter ceramic beads and eight 4 mm diameter glass beads (as recommended by MP-Biomedicals for TeenPrep™ Lysing Matrix E). For the grinding and lysis extraction step, a volume of 8mL of lysis buffer composed of 100 mM Tris-HCl (pH 8), 100 mM EDTA (pH 8), 100 mM NaCl, 20% SDS and ultra-pure water was added in each tube. Mechanical cell lysis was achieved placing the tubes in a FastPrep-24 classic instrument (MP-Biomedicals) set for three runs of 30 s at 4 $m.sec^{-1}$. Tubes were then incubated for 30 min at 70°C to activate chemical lysis and centrifuged at 5000 g for 7 min at 20°C to eliminate particles in suspension. DNA extraction was carried out using 1 ml of supernatant obtained from the centrifugation, as follows: 1) *Deproteinization:* addition of 100 µl potassium acetate 3M pH5.5 to the sample, homogenization and incubation on ice for 15 min to precipitate proteins, centrifugation at 14000 g for 5 min at 4°C to eliminate precipitated proteins (supernatant recovery and pellet disposal); 2) *DNA precipitation:* addition of 900µl cold isopropanol (v/v), gentle agitation of the tubes that were then placed at -20°C for 30 min, centrifugation at 13000 rpm for 30 min at 4°C, elimination of the supernatant; 3) *DNA Washing:* rinsing of the pellet with 400µl 70° cold ethanol, centrifugation at 13000 rpm for 5 min at 4°C, elimination of the ethanol supernatant, drying of the pellet by placing the tubes in a drying oven at 60°C for 20 min; 4) *DNA Purification:* resuspension of the pellet in 500 µl of ultra-pure water. Raw DNA extracts were further purified using a NucleoSpin Soil kit (Macherey-Nagel) following the manufacturer's protocol from step 4 (addition of SL3 buffer). Finally, purified DNA extracts were eluted in 60 µL of buffer and stored at −20°C.

Digital droplet polymerase chain reaction (ddPCR)

To avoid common PCR inhibition problems with the soil matrix and to obtain direct absolute DNA quantification (no standard curve needed), samples were analyzed by droplet digital PCR (ddPCR) using the QX200 ddPCR system (Bio-Rad) composed of a droplet generator, a thermal cycler and a droplet reader. We used the specific PCR primers and TaqMan probe (Giop set) designed by Valsesia et al. (2005) to amplify and mark *P. viticola* DNA in our samples.

For each sample, we added 4 µl of DNA extract diluted to the tenth to 18 µl of a PCR mix composed of 11 µL of 2x ddPCR Supermix for Probes (Bio-Rad), 2.2 µL of 7.5 µM Giop F, 2.2 µL of 7.5 µM Giop R, 2.2 µL of 5 µM Giop P-VIC and 0.4 µL of ultra-pure water. The samples (20 µl) were first placed in the droplet generator to proceed to the breakdown of the samples into 15000 to 20000 micro-droplets using oil. Samples were then carefully transferred to 96-well plates with a pipette, with one sample per well (one single analysis per sample). The sample plates were placed in the thermal cycler for DNA to be amplified according to the following program: 1) an initial phase at 95°C for 5 min; 2) 40 cycles of 30 s at 95°C then 1 min at 60°C then 30 s at 72°C; and 3) a final phase at 98°C for 10 min. Samples were cooled at 12°C before being transferred to the droplet reader for DNA quantification (ratio of positive *vs* negative droplets). Finally, we obtained one value per sample that corresponded to the number of *P. viticola* ITS copies per µl.

Method repeatability assessment

In order to evaluate the repeatability of our method, we conducted additional analyses of soil samples. First, we randomly selected 44 soil samples out of the 317 samples that we collected in the experimental vineyard. For each of these samples, we took three portions of 2 g from the electric mixer bowl after the homogenization

step. DNA was extracted from each portion separately, then the three portions were analyzed via ddPCR separately but at the same time (same operator, same day, same plate, and same machine run). The three portions of a sample were considered as extraction replicates (keeping in mind that the subsampling step's repeatability depends on the quality of sample homogenization). Next, we randomly selected another 42 soil samples from our collection. After a single DNA extraction per sample, we repeated the ddPCR analysis for three 4 µl aliquots of the DNA extraction product (previously diluted to the tenth) for each sample. The three aliquots of a sample were considered as ddPCR replicates. For both DNA extraction and ddPCR replicate data, we fit an analysis of variance model for the number of ITS copies as a function of the sample. In each case, we compared the residual variance (within-group variance, *i.e.* here the variance between replicates of a sample) to the variance explained by the model (between-groups variance, *i.e.* here the variance between samples) using an F-test, to evaluate the ability of our method to provide repeatable measures. In addition, we computed the coefficient of variation of the measurements associated with either DNA extraction or ddPCR as the ratio between the within-group standard-deviation (root square of the residual variance; expressed in the same unit as the response variable) and the mean number of ITS copies. The coefficient of variation indicates the mean dispersal of the values obtained for the replicates of a sample compared to the mean of all values, and a method is considered to have good repeatability when the coefficient of variation is inferior to 10%.

Estimation of ITS copy number in Pv genome

In order to estimate the ITS copy number in the genome of *P. viticola*, we compared the ddPCR signals obtained with the ITS primers (Valsesia et al. 2005) *vs* primers targeting the single copy β-tubulin gene (Weerakoon et al. 1998). First, zoospores of seven *P. viticola* strains frequently used in laboratory for genetic applications were collected with a paintbrush from grapevine leaves infected beforehand on purpose and placed into separate 2 mL microcentrifuge tubes with 1 mL Tris-EDTA buffer. Second, freeze-dried samples were extracted following a SDS based method and DNA quantity and quality were checked by dosage with either Qubit 4 or Denovix-11. About 35 sequences from NCBI (Fontaine et al. 2021; Rouxel et al. 2013) were aligned with *P. viticola* genome using Geneious Prime. Primers (Forward: ACAGCCAATTTTCGTAAGTCC, Reverse: GCCTTGTACGACATTTGCTTT) and a TaqMan probe (5' FAM-TGTCCGGGAAATCGAAGGCA-MGB 3') were designed using the consensus sequence with 100% similarity. Specificity was tested using NCBI Blast (blast.ncbi.nlm.nih.gov) and by running quantitative PCRs on either pure *P. viticola* strain, *P. viticola* with grapevine leaf or grapevine leaf only (see Figure S1 in Supplementary Materials) using a QuantStudio 5 (Life Technologies). Reaction mix was composed of 10 µL of 2X PCR Buffer (Takyon Low Rox Probe MasterMix - Eurogentec), 1,6 µL of each primer at 10 µM, 0,4 µL of probe at 10 µM, 3,9 µL of molecular biology water (Sigma) and 2,5 µL of DNA template for a 20 µL final volume. Due to a large copy number difference between both genes and ddPCR sensitivity, we run the reactions for each marker in separate reaction wells. In consequence, each sample were normalized with a final quantity of 5 pg for ITS samples and 5 ng for β-tubulin samples. All reactions were run with a cycling program starting with 3 min at 95°C followed by 40 cycles of 10 s at 94°C alternating

with 60 s at 60°C. For each strain, the number of ITS copies was estimated as the ratio of β-tubulin to ITS copy number per ng.

Spatial structure of Pv primary inoculum in a vineyard

The spatial structure of *P. viticola* primary inoculum in the experimental vineyard was investigated on both a field-scale and a plot-scale by analyzing the regular grid data and the nested sampling plots data, respectively, using a geostatistical approach. Hereafter, we describe the field-scale analysis only, but the same methodology (except model fitting and kriging) was applied for the plot-scale analysis. Details on the plot-scale analysis are available in Supplementary Materials (Tables S2 and S3; Figures S2).

Plasmopara viticola DNA in soil samples, expressed as the number of ITS copies per µl of extraction product, was log-transformed before analysis to reduce the skewness of the distribution and limit variance inflation and variogram distortion (Oliver and Webster 2014). First, all pairs of data (N=19503) were segregated into distance classes. The maximal distance between two points in our dataset was 65.09 m. In our analysis, however, we considered a maximal separation distance of 60m to exclude highest distance classes with a number of point pairs below the empirical threshold for semivariance estimates accuracy (at least 30 to 50 pairs required; Chiles and Delfiner, 1999; Journel and Huijbregts, 1976). We considered a spatial lag of 2m, which led to a total of 29 distance classes, with 79 to 1498 pairs each. The sampling points in the first distance class were separated by a median distance of 3.02 m. We then computed the semivariance for each distance class using the Matheron estimator (Matheron 1963), defined as follows:

$$\gamma(h) = \frac{1}{2n(h)} \sum_{i=1}^{n(h)} [z(x_i) - z(x_{i+h})]^2,$$

where $z(xi)$ is the primary inoculum at the first point of the ith pair, $z(xi + h)$ is the primary inoculum at the second point of the ith pair, h is the median of the class of distance considered and n is the number of point pairs in the distance class considered. We represented the omnidirectional experimental semivariogram of the primary inoculum of *P. viticola* in the vineyard by plotting the semivariance against the sampling point separation distance h. A semivariogram shows how the similarity between samples changes with increasing separating distance *i.e.* spatial dependence. It can take various forms, and semi-variance often increases with distance until it reaches a plateau at which point it remains stable. The variogram is flat in the absence of spatial structure.

A visual inspection of the experimental semivariogram allows one to determine its general shape. We fitted a spherical model (linear-sill shape) to the experimental semivariogram using ordinary least square residuals method (Cressie 1985). The spherical model is as follows:

$$\gamma(h) = C_0 + C\left(\frac{3h}{2a} - \frac{1}{2}\left(\frac{h}{a}\right)^3\right) \quad 0 < h \leq a$$

$$\gamma(h) = C_0 + C \quad h > a$$

The model parameter estimates were regarded as quantitative descriptors of the spatial pattern of the data. They included i) the spatial range a, or the distance beyond which variance is constant; ii) the nugget variance C_0, an estimate of error measurement plus error due to uncontrolled variability at distance lags shorter than

the shortest lag considered; iii) the structural variance C; and iv) the sill $C_0 + C$, or sample variance.

We used the shape and parameter estimates of our semivariogram model to interpolate *P. viticola* primary inoculum values at unsampled locations over a 0.05 m × 0.05 m grid by ordinary kriging, which is an optimal interpolation procedure described in detail in various sources (*e.g.* Goovaerts, 1998; Oliver and Webster, 2015). After back-transforming the resultant values, we produced a contour map of the spatial distribution of the primary inoculum in the field, as interpolated from our data (*i.e.* given the local conditions and our sampling plan).

All geostatistical analyses were performed using the package gstat (Pebesma 2004) in the R statistical software (v4.3.1, R Core Team, 2023). The contour map was designed using the ggplot2 package (Wickham 2016).

Comparison with spatial patterns in soil moisture and grapevine vigor

A private company (GEOCARTA) assessed soil electrical resistivity (SER) in the experimental vineyard in May 2006 using an ARP© system (see Andrenelli et al., 2013 for a detailed description of the device) which provided one measurement every 0.2 m along transects parallel to the rows. One measurement corresponded to the average of the electrical resistivity from the surface to 50 cm depth, *i.e.* apparent electrical resistivity. The raw data were first processed by 1D median moving window filtering along the acquisition profiles to eliminate noise in the measurements. Then, the dataset was interpolated in two dimensions on a 2-m square grid (2D bicubic spline interpolation) by the company. We proceeded to a second, finer-scale interpolation so that final SER data corresponded to predicted values on a 0.1-m

grid. Soil electrical resistivity (the opposite of electrical conductance) is expected to decrease with increasing water content, as the charged ions in water make it highly electrically conductive. Therefore, we considered SER to reflect the inverse of soil moisture and we hypothesized that the distribution of primary inoculum was negatively related to the distribution of SER (and positively to soil moisture). We assumed that soil physico-chemical properties that control SER did not change significantly between the SER (2006) and inoculum measures (2022).

A GreenSeeker^{TM} optical captor was used to assess the normalized difference vegetation index (NDVI) of the foliage in the experimental vineyard during the growing season preceding soil sampling (*i.e.* June 2021). The optical captor was installed on a tractor and recorded one measure every 0.2m along each row (see Goutouly et al., 2006 for a detailed description). NDVI is a widely accepted indicator of vegetative biomass and plant vigor, which we surmised to be related to downy mildew susceptibility.

We investigated the relationship between spatial patterns in DM primary inoculum, SER and NDVI using cross variograms. First, we calculated a unique SER and a unique NDVI value for each primary inoculum sampling point of the regular grid as the mean of SER values within a 0.95 x 0.8m rectangle around each sampling point, and the mean of NDVI values within 0.48m of each sampling point, respectively. We reduced the skewness of the distribution of both SER and NDVI calculated data by applying a box-cox power transformation to each variable (Box and Cox 1964; Zhang et al. 1998). The interdependence between primary inoculum and SER or NDVI was examined using experimental cross-variograms, estimated by the following:

$$\hat{\gamma}_{uv}(\mathbf{h}) = \frac{1}{2m(\mathbf{h})} \sum_{i=1}^{m(\mathbf{h})} [\{z_u(\mathbf{x}_i) + z_u(\mathbf{x}_i + \mathbf{h})\} \{z_v(\mathbf{x}_i) + z_v(\mathbf{x}_i + \mathbf{h})\}].$$

where $m(h)$ is the number of comparisons at lag h; $z_u(x_i)$ and $z_u(x_i + h)$ are the measured values of the variable z_u; $z_v(x_i)$ and $z_v(x_i + h)$ are the measured values of z_v at x_i and $x_i + h$, respectively. A positive relationship between the cross semivariance and distance lag indicated a positive coregionalization between both variables.

Pv primary inoculum along depth and distance-to-row gradients

In the nested sampling plots, the sampling points were located either below the vine stocks in the row (10 samples per plot) or in the inter-row space at 20, 60 or 80 cm from the nearest row (respectively 4, 4 and 10 samples per plot). We used this data to fit a generalized linear model (Poisson error distribution) testing whether the amount of primary inoculum in the soil varied along a gradient of distance to the row. We included the plot as a random intercept effect in the model to account for the dependence of the data within the plots. We fitted another generalized linear model (Poisson error distribution) to our depth sampling data to test whether the amount of Pv primary inoculum varied between soil layers. We included the sampling location (n=6) as a random intercept effect in this second model to account for the dependence of the data at one location.

A bioassay to assess soil infectious potential

The principle of the bioassay is to place soil samples in optimal temperature and humidity conditions for oospore germination, to trap the released zoospores using susceptible grapevine leaf discs, and finally to approximate the infectious potential by evaluating the extent to which leaf discs are infected.

We performed the bioassay on one fourth of our soil samples (n=40) using a 1 g portion per sample. Each sample was placed in the bottom of a 10 cm diameter circular plastic box half-filled with osmosed water and incubated at 20°C in the dark to stimulate oospore germination. We collected leaves from untreated Cabernet Sauvignon grafted plants grown in greenhouses. We specifically picked the third or fourth leaves from the apex, as leaves at this stage of development are particularly susceptible to downy mildew infection (Isabelle Demeaux, personal communication). We cut 10mm diameter discs in the leaf blade with a manual round cutter. On the first day of the incubation (day 0), we placed 10 discs from 10 different leaves (to avoid biases due to differences in downy mildew susceptibility between leaves) on the surface of the water (abaxial face down) in each box. The leaf discs were used to trap the zoospores released into the water following germination of oospores present in the soil sample, *i.e.* the zoospores swam to the leaf discs and infected them via the stomata. After 48 h, we placed the 10 discs abaxial face up on a moist Whatman® filter paper sheet in a transparent box sealed with plastic film (to maintain high humidity) and incubated at 20°C with a 12h-12h day-night light cycle for 6 days. After 6 days of incubation, we visually inspected the discs and evaluated the percentage of the area covered with *P. viticola* sporangiophores for each disc. The germination of a cohort of oospores under optimal conditions (immersed in water, in the dark and at 20°C) extend over 6 to 8 days, with a peak around the second and third days of incubation. To account for germination dynamics, we repeated

zoospore trapping using leaf discs on day 2, 4 and 6 from incubation start. We used the cumulative number of infected discs and the mean percentage of leaf area infected as indicators of the infectious potential of the soil.

We assessed the relationship between the abundance of primary inoculum in the soil (as estimated with the ddPCR approach) and soil infectious potential by fitting one generalized linear model per indicator (Poisson error distribution in both cases) with the number of *P. viticola* ITS copies per µl as a predictor. We computed the McFadden's pseudo R^2 of the two models to determine the indicator best fitting the primary inoculum data.

Results

DNA extraction and ddPCR repeatability

From the set of 44 samples randomly selected for DNA extraction repeatability assessment (Figure 2), we found 12.23 ITS copies per µl on average with a within-sample standard deviation of 4.60 ITS copies per µl. The analysis of variance indicated that the residual variance (within-sample variance S_{WS}=21.12; associated to measurement error) was significantly lower than the explained variance (between-sample variance S_{BS}=159.26 ; F=7.54; p=1.40 10^{-16}) meaning that the error of measurement associated with our DNA extraction method was low compared to the between-sample variability. The within-sample coefficient of variation (*i.e.* associated with the repeated measurements of a sample) was equal to 41.2% on average, and varied from 7% to 160%.

From the 42 samples that were selected for the assessment of ddPCR repeatability (Figure 2), we obtained 11.83 ITS copies per µl on average, with a within-sample

standard deviation of 2.68 ITS copies per µl. The analysis of variance indicated that the residual variance (S_{WS}=7.17) was significantly low compared to the explained variance (S_{BS}=334.01; F=46.59; p=1.09 10^{-40}). The within-sample coefficient of variation (*i.e.* associated with the repeated measurements of a sample) was equal to 26.5% on average, and varied from 1% to 173%.

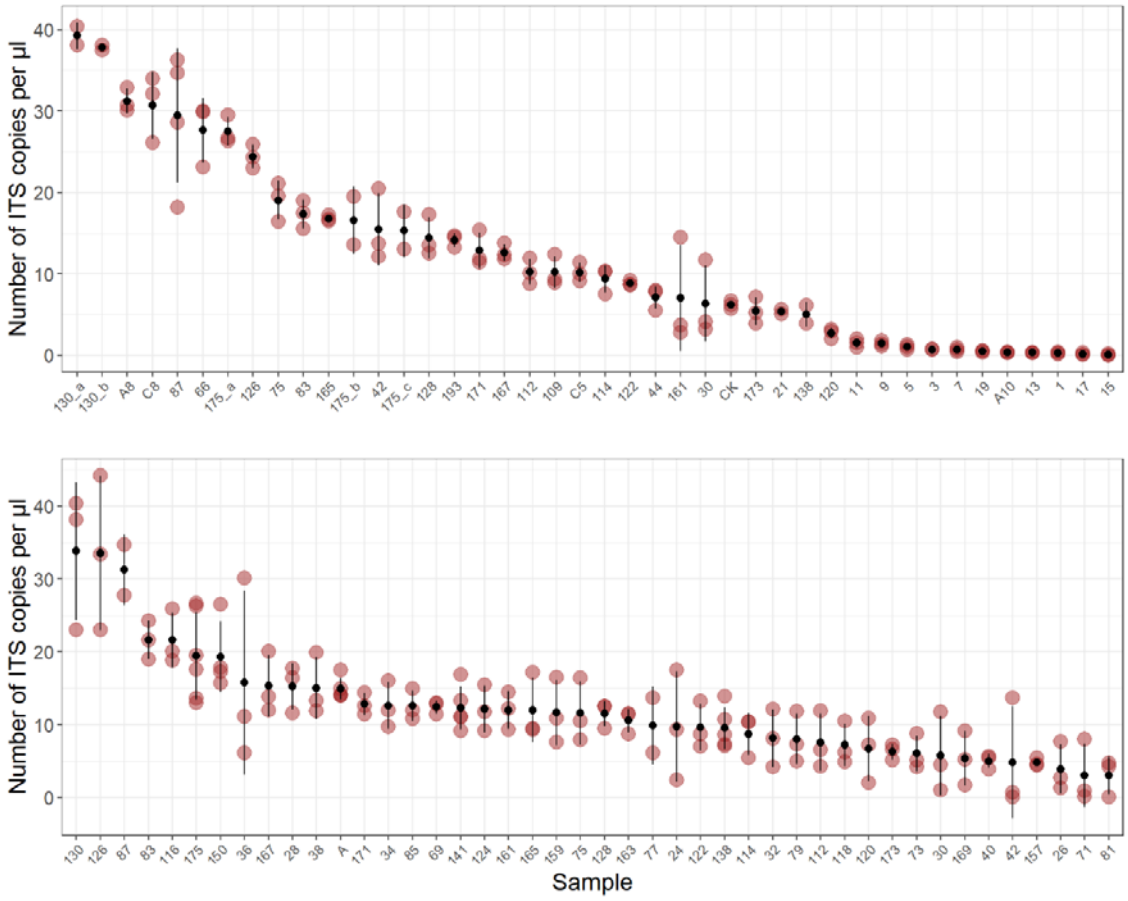

Figure 2. Triplicates of DNA extraction for 44 randomly selected soil samples (upper panel). Triplicates of ddPCR amplification for 42 randomly selected DNA samples (lower panel). Red dots correspond to repeated measurements of the number of ITS copies per µl found in the samples. Black dots and bars correspond to within-sample mean and standard deviation of the number of ITS copies per µl, respectively.

<u>Quantification of Pv primary inoculum in vineyard soil samples</u>

Considering the regular grid and nested sampling plot data, we found *P. viticola* DNA in all samples except one, with 6.62 ± 6.68 ITS copies per µl on average. The value for positive samples varied from 0.05 to 40.4 ITS copies per µl. A map of the raw data is available in Supplementary materials (Figure S3).

By comparing the ITS to the β-tubulin signal obtained by ddPCR for seven *P. viticola* strains, we found that the genome of *P. viticola* contains on average 204 ± 37 copies of the ITS sequence (see Table S1 in Supplementary Materials for details). Using this value, we estimated that there was on average 5.84 ± 5.90 oospores per gram of soil in the experimental vineyard (up to 35.65 oospores per gram of soil; see Figure S5 in Supplementary materials for computation details).

Spatial structure of Pv primary inoculum in a vineyard

After log-transformation, the skewness of the distribution of *P. viticola* DNA data was reduced from 1.69 to -0.35 for the regular grid, and from 2.40 to 0.42 for the nested sampling plots. The shape of the fitted spherical model (regular grid data) revealed that the downy mildew primary inoculum was spatially structured at the field scale (Figure 3). The range was 25.8m. The nugget variance, the structural variance and the sill were 0.36, 0.27 and 0.61 respectively. The high nugget value indicated that very close points could be quite dissimilar in terms of primary inoculum, suggesting the existence of a source of variation operating at a scale finer than that of the regular grid. The map of the values interpolated by kriging using the fitted model is shown in Figure 3.

The pattern of the plot-scale experimental semivariogram was not typical, with semivariance alternatively increasing and decreasing along the gradient of

separation distance (Figure S2 in Supplementary Materials). Semivariance peaks corresponded to distance classes with a higher proportion of heterogeneous pairs of points, *i.e.* pairs consisting of one sampling point in a row and one sampling point in an inter-row. On the other hand, lowest semivariance values corresponded to distance classes with a higher proportion of homogeneous pairs of points, *i.e.* pairs with two sampling points in a row or pairs with two sampling points in an inter-row (Figure S2 in Supplementary Materials). We consistently found that semivariance was higher for heterogeneous pairs of points than for homogeneous ones, on average (anova P <0.0001, Figure S2 and Table S3 in Supplementary Materials).

Figure 3. Empirical semivariogram of downy mildew primary inoculum in the soil of the experimental vineyard (bottom left panel; open circles size is proportional to the number of data pairs; solid line corresponds to the fitted spherical model). Map of the experimental vineyard with interpolated values of downy mildew primary inoculum (right panel), expressed as the number of ITS copies per µl.

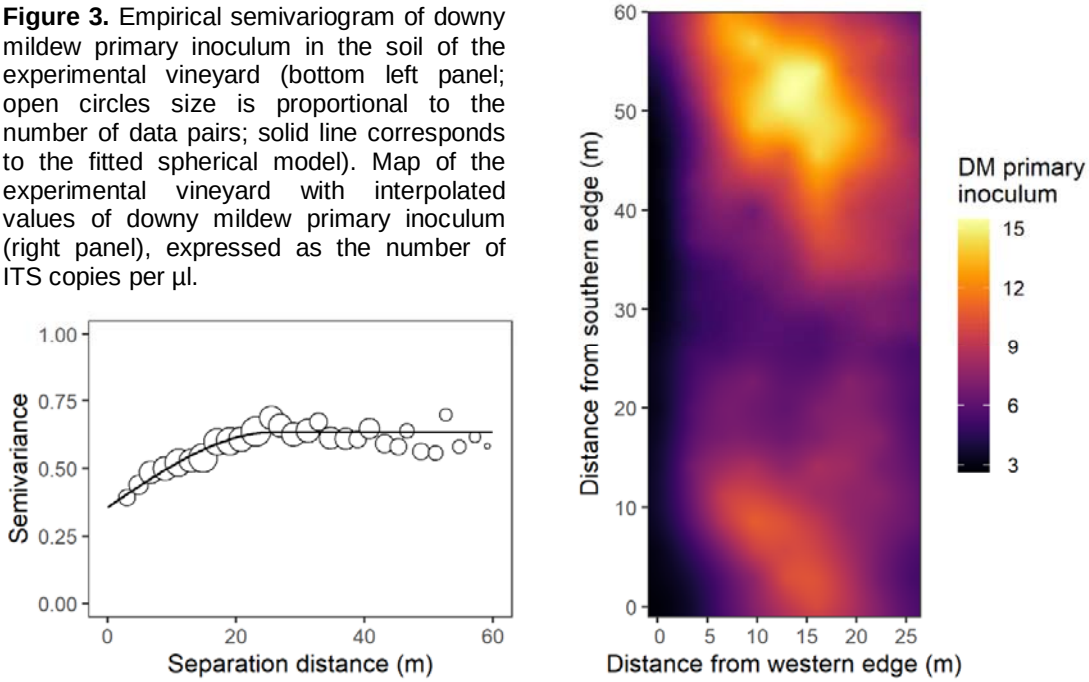

Comparison with spatial patterns in soil moisture and grapevine vigor

The cross-variograms revealed a clear negative coregionalization between downy mildew primary inoculum and SER (Figure 4), or alternatively a positive

coregionalization with soil moisture. This result is consistent with our hypothesis that soil moisture promotes disease incidence locally, which in turn explains local inoculum accumulation.

The cross-variogram of downy mildew primary inoculum *vs* grapevine vigor did not indicate a clear coregionalization of the two variables (Figure 4; weak positive correlation up to 25 m of distance then weak negative correlation). This result did not support our hypothesis for a cascading effect of vigor on local disease incidence (due to greater susceptibility).

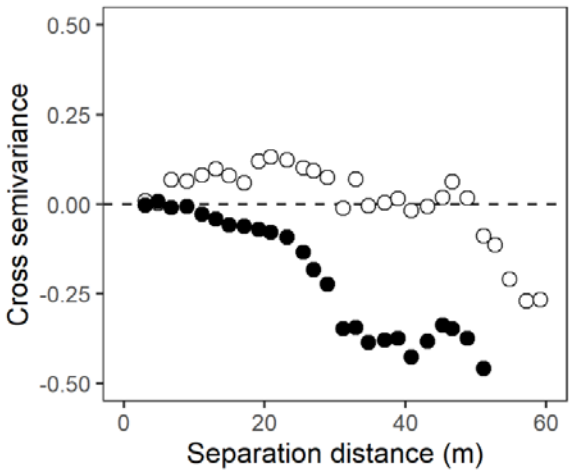

Figure 4. Cross-variograms of downy mildew primary inoculum *vs* soil electrical resistivity (black) or grapevine NDVI (white).

<u>Pv primary inoculum along depth and distance-to-row gradients</u>

Our results clearly indicated that there was a decreasing gradient of primary inoculum from the row to the middle of the inter-row (Figure 5; $\beta = -0.0280 \pm 0.0002$; $P < 0.001$). Downy mildew primary inoculum was five to six times more concentrated in the ridge of soil below the vine stocks (in the “cavaillon”; 9.32 ± 6.32 ITS copies per µl) than in the inter-row space (1.72 ± 1.66 ITS copies per µl), on average. These

results were in line with the results from the geostatistical analysis of nested sampling plot data (see above). We also found that the primary inoculum concentration decreased with soil depth ($\beta = -0.1529 \pm 0.0071$; $P < 0.001$). The primary inoculum appears to mostly accumulate in the first 10 centimeters of soil and was barely detected below this depth (Figure 5).

Although we were not seeking to address this point, we also found that primary inoculum concentration in the soil varied between rows, with significantly less *P. viticola* DNA on average in the westernmost row compared to others in the vineyard (Figure S4 Supplementary Materials; $F = 6.522$; $P < 0.001$; see Table S4 in Supplementary Materials for results of Tukey's multiple comparison test). This unexpected result was consistent with the distribution of primary inoculum as predicted by kriging of observed data (Figure 3).

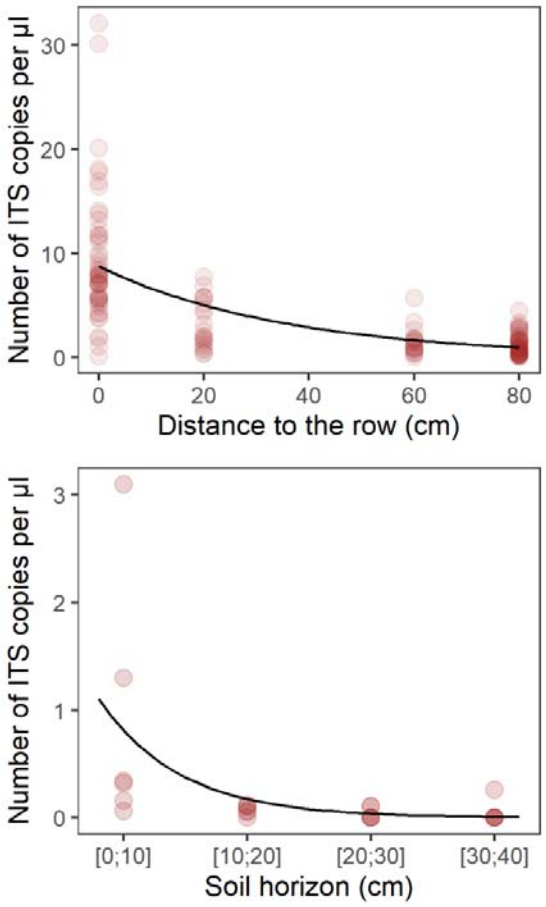

Figure 5. Abundance of downy mildew primary inoculum (as number of ITS copies per µl estimated by ddPCR) along gradients of distance to the row (upper panel) and soil depth (lower panel). Solid lines correspond to model predictions.

A bioassay to assess soil infectious potential

We found that soil infectious potential, as assessed with our bioassay, was explained by downy mildew soil primary inoculum. The cumulated number of leaf discs infected by DM from 1g of soil sample over the duration of the assay varied from 0 to 12 discs (out of 40). The average proportion of disc area covered with *P. viticola* sporulation varied from 0 to 10.3%. The cumulated number of infected discs significantly increased with the number of ITS copies per µl (Figure 6; □ = 0.029 ± 0.008 ; P <

0.0001 ; McFadden's pseudo R^2 = 0.05). In addition, the average infected area significantly increased with the number of ITS copies per µl (Figure 6; □ = 0.06 ± 0.01; P < 0.0001 ; McFadden's pseudo R^2 = 0.16).

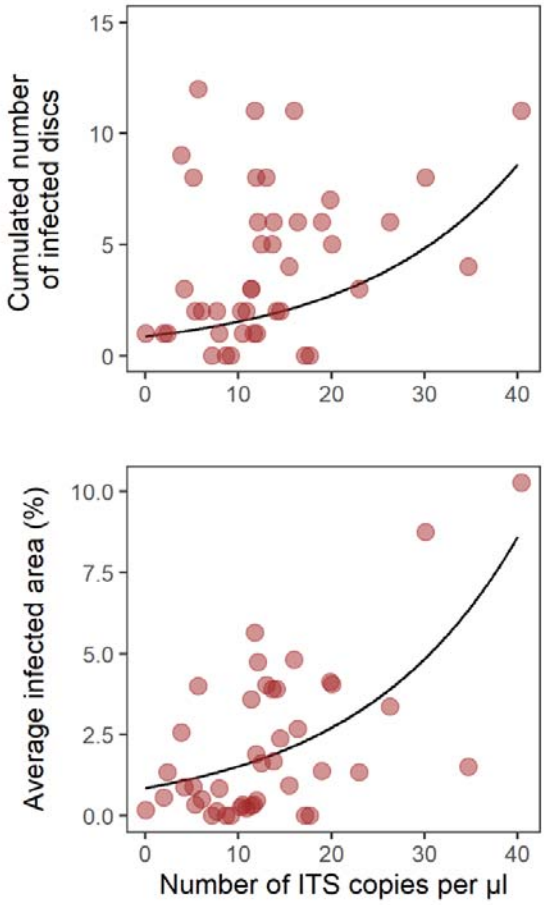

Figure 6. Comparison of bioassay and digital droplet PCR. Relationships between the abundance of DM primary inoculum in the soil (measured as number of ITS copies per µl by ddPCR) and the infectious potential of the soil measured by a bioassay, as either the cumulated number of infected discs (upper panel) or the average trap disc infected area (lower panel). Solid lines represent fitted model predictions.

Discussion

For the first time, we were able to produce an image of the spatial distribution of the reservoir of DM primary inoculum in the soil of a vineyard at the onset of the growing season. This was made possible due to the development of a new and repeatable method for the quantification of *P. viticola* DNA from soil samples. This tool enables us to provide quantitative insights into the sexual cycle of *P. viticola* in the soil

compartment and improve our understanding of downy mildew epidemiology. In this study, we used this method to describe the spatial distribution of downy mildew primary inoculum at different spatial scales. The study of disease inoculum abundance and spatial distribution in agricultural soils are generally restricted to soilborne pathogens, including oomycetes (see for example Botero-Ramirez et al., 2021; Moussart et al., 2009). To our knowledge, these questions have rarely been addressed regarding airborne pathogens with a dormant telluric stage, since the emphasis is generally on the management of the pathogen during its active phase in the aboveground compartment where it attacks plants. However, we believe that the knowledge gained from a study like this one will be crucial to shift toward preventive management strategies.

Plasmopara viticola was encountered at all sampled locations in the field contrary to soilborne pathogens whose presence is generally restricted to some areas (Botero-Ramirez et al. 2021; Moussart et al. 2009). This difference may be explained by the greater dispersal ability of the airborne form of *P. viticola* resulting in greater propagation of the disease, as well as to the redistribution of inoculum contained in leaf litter blown by the wind. Still, we showed that the distribution of downy mildew primary inoculum was not random or regular on a field scale, but that it was characterized by 25 m-diameter patches of concentrically increasing oospore concentration, suggesting that aerial dispersion did not fully homogenize inoculum abundance. We further demonstrated that this distribution pattern could be indirectly determined by the spatial variability of some abiotic factors that control disease incidence. Indeed, we showed that the concentration of primary inoculum in the soil was positively coregionalized with soil moisture. It has been established that soil moisture was also one of the main factors explaining soilborne disease occurrence

(Jiang et al. 2021). These findings support the hypothesis of local accumulation of inoculum, *i.e.* the amount of inoculum formed in a given area in a field is proportional to disease incidence, then leaves fall and remain close to the vine they fell from and oospores are unlikely to disperse once in the soil matrix. As mentioned above, this local accumulation pattern can be reinforced by soil ridging. The absence of a clear relationship with grapevine vigor may be due to several reasons. Contrary to soil physical characteristics, grapevine vigor is dependent on many factors and may vary rapidly during the course of the growing season. Therefore, it is more difficult to establish a relationship between grapevine vigor and accumulated inoculum in the soil, especially as we tried to relate a discrete assessment of vigor with an assessment of downy mildew primary inoculum that reflects disease severity integrated over the whole season. Second, the detection of a relationship between grapevine vigor and primary inoculum concentration may have been mitigated by the phytosanitary treatments applied in the experimental field during the 2021 growing season. Therefore, grapevine vigor or foliage density cannot be used to predict DM primary inoculum distribution, and controlling for vigor is not a promising lever for DM primary inoculum management unless further research establishes a stronger relationship.

We found that the primary inoculum for downy mildew epidemics (*i.e.* oospores) accumulates preferentially in the ridge of soil below the vine stocks (or “row location”) at a rate of 4 to 5 times the inter-row space, and in the first 10 cm of soil, where it is more likely to reach the host tissue in the event of rain splashes. Although primary inoculum concentration varied on a wider spatial scale within the field (25m patches), this row vs inter-row contrast was observed at all locations in the field. Moreover, primary inoculum concentration was more similar at two row locations

whatever the distance between the two points than when comparing row *vs* inter-row locations. It suggests that the distribution of primary inoculum is partly determined by cultural choices, such as row and vine spacing, and the spatial variation of cultural practices related to it (*e.g.*, tillage under the vine *vs.* vegetation cover between the rows). *Plasmopara viticola* oospores are dispersed as “hitchhikers” in host leaves and, exactly as in annual crops, grapevine leaves can be seen as crop residues carrying disease inoculum. Tillage can modify the spatio-temporal distribution of crop residues (Guérif et al. 2001). The development of phoma stem canker (caused by the fungus *Leptosphaeria maculans*) in oilseed rape crops is prevented by ploughing stubble after harvest to limit the production of primary inoculum (*i.e.* ascospores) on infected residues. However, a study showed that stubble was brought back to the surface at the time of tillage and sowing (Schneider et al. 2006). In a corn field, ridges formed by tillage prior to crop sowing were found to contain higher proportion of organic matter than furrows due to redistribution of residues in decomposition (Grigera et al. 2007). Here, we hypothesize that soil ridging at the foot of the vines in the autumn “traps” the fallen leaves, keeping the oospores in the ground by covering them or by preventing wind dispersion, resulting in a higher concentration of inoculum locally. Future research should study the fate of grapevine leaf litter (or crop residues) during winter as affected by cultural practices to better understand oospores distribution in vineyards and identify cultural practices that prevent inoculum from accumulating in the vineyard below the grapevines.

Interestingly, our study reveals that soil oospore concentration can vary between rows within a field and be subjected to border effects. Indeed, we found that the primary inoculum was 7 to 8 times less concentrated in the westernmost row compared to the rest. This difference might arise from various mechanisms mediated

by the presence of a tree hedgerow alongside the experimental field. In agricultural landscapes, tree hedges provide multiple ecosystem services, including wind erosion in particular on the leeward side of the hedge, up to a distance proportional to hedge height (Campi et al. 2009; Jacobs et al. 2022; Weninger et al. 2021). Wind erosion is generally accompanied by increased air temperature and relative humidity as compared to the conditions in the center of the field (Campi et al. 2009; Jacobs et al. 2022). In spite of many positive effects of hedges on soil fertility, they may have negative effects on crop yield due to competition for resources. Grapevine vigor and yield were found to be reduced up to 4m of the hedge by high levels of competition for nutrients between the crop and the trees of the hedgerow (Favor and Udawatta, 2021; but see Bourgade et al., 2020). In summary, the effect of the hedgerow on soil oospore concentration could arise from three mechanisms : i) windstop or barrier effects that modify leaf litter dispersion on the ground during autumn and winter; ii) microclimate modification in the vicinity of the hedgerow that modulates disease incidence locally; iii) modulation of grapevine vigor and susceptibility to DM due to competition for resources. In our case, the absence of a border effect on the east side of the field (also bordered by a hedgerow) suggests that mechanisms at play operate asymmetrically. We hypothesize that leaves on the ground are mostly carried from west to east by the prevailing westerly winds in the zone (i.e. orthogonally to rows). Leaves coming from neighboring fields that would enter the field by the west border may be stopped by the hedgerow (*i.e.* barrier effect), explaining the inoculum depletion in the first row. In any case, these results underline the importance of understanding leaf litter dispersal at fall, and raise questions regarding the effects of agroecological infrastructures on downy mildew

epidemiology, as well as their contribution to preventive disease management strategies.

Our method for inoculum assessment is based on the ddPCR technique, which is particularly well suited for rare targets in complex matrices because of the partition of the samples into thousands of droplets that dilutes both DNA and inhibitors and improves the yield of amplification and the sensitivity of the analysis as compared to qPCR, including in the case of oomycete quantification in soil samples (Gossen et al. 2019; Rački et al. 2014; Wen et al. 2020). In addition, the use of an ITS sequence occurring in numerous copies increases the probability of detection when *P. viticola* is present in small quantities in the sample. As a first step towards the epidemiological interpretation of our ddPCR results, we converted the number of ITS copies into a number of oospores per gram of soil after estimating the occurrence of the target ITS sequence in the genome of *P. viticola*. We estimated that there was 5 to 6 oospores per gram of soil on average. The number of ITS copies we found (204) is consistent with what was found for other oomycetes (95 copies per haploid genome on average; Gangneux et al., 2014) and the conversion of ddPCR number of ITS copies into the number of oospores has been used for other soilborne oomycetes (Chatterton et al. 2023). However, we may underestimate soil oospore concentration due to suboptimal DNA extraction and amplification yields, which need to be assessed. Moreover, our estimation of the number of ITS copies was obtained from a reduced panel of seven *P. viticola* strains, which may not be fully representative of the intra-specific variability. Further analyses should be undertaken to better assess the occurrence of the ITS sequence on a population level, given that soil samples collected from the vineyard potentially contain a high diversity of strains. In addition, studies aimed at describing the genetic structure and diversity of *P.*

viticola populations in the soil compartment would help refine our evaluation of soil oospore concentration.

Using an original bioassay, we were able to demonstrate that the concentration of *P. viticola* oospores in the soil is related to soil infectious potential (as estimated in controlled conditions using a leaf disc bioassay), meaning that our DNA-based quantification of primary inoculum can have an epidemiological significance. In *Aphanomyces euteiches*, the causal agent of pea root rot, inoculum potential estimated from soil samples using trap seedlings was positively related to disease severity observed on peas during the cropping season (Moussart et al. 2009). Hwang et al. (2011) found similar results regarding canola clubroot disease, which is caused by another soilborne oomycete, but we found no study that addressed the inoculum density-disease severity relationship for soil-to-aerial plant parts infection pathway. The relationship found between primary inoculum concentration in the soil and our indicator of infectious potential suggests that any measure reducing the accumulation of primary inoculum in a field could result in lower epidemic pressure. Such measures could include tactical actions taken over the short-term, such as the removal of infected leaves (*i.e.* inoculum reservoir) from one season to the next (in autumn) or the modification of crop implantation and/or soil management practices to reduce physical barriers (*e.g.* ridge, microtopography) that could impede wind dispersal of leaves outside the field. Further studies should evaluate the efficacy of these kinds of measures aiming at reducing levels of initial inoculum to control disease impact on crops.

Prophylactic measures aimed at limiting primary inoculum accumulation in the vineyards will have synergistic effects with other disease management strategies. By

lowering the epidemic pressure, they could make the use of biocontrol or biostimulation products more attractive. The probability of a resistance breakdown in a pathosystem depends on the evolutionary potential of the pathogen which is affected by many factors including the size of the pathogen population (Aubertot et al. 2006). By removing the products of sexual reproduction (*i.e.* oospores), prophylactic practices could also slow down resistance breakdown and improve the sustainability of resistant varieties, which was previously suggested (Bitencourt et al. 2021). This was experimentally demonstrated in apple orchards where it was found that the removal of leaf litter in autumn together with spraying of fungicides in the case of moderate or high risks of scab infection delayed the breakdown of the major resistance Rvi6 of Ariane by virulent isolates (Didelot et al. 2016).

As agriculture moves away from chemical biocides, the design of sustainable, adaptative and cost-effective crop disease management strategies will rely more and more on the prevention of epidemic risks and a predictive evaluation of pathogen population dynamics. In this context, the quantitative and spatially-explicit survey of inoculum reservoirs is crucial. The insights gained into DM epidemiology from our methods will contribute to the design of tailored measures aimed at preventing primary inoculum accumulation in the vineyard from one season to the next.

Acknowledgements

The authors would like to thank the SEVEN Mixt Technologic Unit for building and initiating the PROFIL project (see Fundings section). The authors also thank the Experimental Viticultural Unit of Bordeaux 1442, INRAE, F- 33883 Villenave d'Ornon, for the maintenance of the experimental vineyard that was used in this study, and the GenoSol platform (DOI 10.15454/L7QN45) for sharing its expertise and helping with

methodological development for DNA extraction from soil samples. Part of the experiments (ddPCR analysis) were performed at the Genome Transcriptome Platform of Bordeaux (PGTB; doi:10.15454/1.5572396583599417E12) with the help of Adline Delcamp and Emilie Chancerel. Finally, the authors are grateful to the sponsors of the Chaire Alexis Millardet for their support to research activities, namely Château Ausone, Château Cheval Blanc, Petrus and Château Montrose.

Fundings

This work was initiated thanks to the Ministries for an Ecological Transition, for Agriculture and Food, for Solidarity and Health and of Higher Education, Research and Innovation, with the financial support of the French Office for Biodiversity, as part of the call for research projects “Overall approaches to limit the use of phytosanitary products : coupling preventive and curative solutions within agricultural sectors from farmers to consumers”, with the fees for diffuse pollution coming from the Ecophyto II+ plan (PROFIL project 2020-2024). This work was also financially supported by the ISVV Fund of the Fondation Bordeaux Université, through the Chaire Alexis Millardet program. The authors acknowledge the financial support of the French National Research Agency (ANR) under the grant 20-PCPA-0010 (PPR VITAE). The GenoSol platform (DOI 10.15454/L7QN45) of the infrastructure ANAEE-Services received a grant from the French state through the National Agency for Research under the program “Investments for the Future” (reference ANR-11-INBS-0001), as well as a grant from the Regional Council of Bourgogne Franche Comté. The BRC GenoSol is a part of BRC4Env (10.15454/TRBJTB), the pillar « Environmental Resources » of the Research Infrastructure AgroBRC-RARe 10.15454/b4ec-tf49.

Literature Cited

Andrenelli, M. C., Magini, S., Pellegrini, S., Perria, R., Vignozzi, N., and Costantini, E. A. C. 2013. The use of the ARP© system to reduce the costs of soil survey for precision viticulture. Journal of Applied Geophysics. 99:24–34.

Aubertot, J. N., West, J. S., Bousset-Vaslin, L., Salam, M. U., Barbetti, M. J., and Diggle, A. J. 2006. Improved resistance management for durable disease control: A case study of phoma stem canker of oilseed rape (*Brassica napus*). In *Sustainable strategies for managing Brassica napus (oilseed rape) resistance to Leptosphaeria maculans (phoma stem canker)*, eds. B. D. L. Fitt, N. Evans, B. J. Howlett, and B. M. Cooke. Dordrecht: Springer Netherlands, p. 91–106. Available at: https://link.springer.com/10.1007/1-4020-4525-5_8 [Accessed June 16, 2024].

Beaumelle, L., Tison, L., Eisenhauer, N., Hines, J., Malladi, S., Pelosi, C., et al. 2023. Pesticide effects on soil fauna communities—A meta-analysis. Journal of Applied Ecology. 60:1239–1253.

Beketov, M. A., Kefford, B. J., Schäfer, R. B., and Liess, M. 2013. Pesticides reduce regional biodiversity of stream invertebrates. Proc. Natl. Acad. Sci. U.S.A. 110:11039–11043.

Bitencourt, C., Pierre, P. M. O., Pinto, F. A. M. F., Fermino-Junior, P. C. P., Gomes, B. R., De Morais, A. C., et al. 2021. First report of oospore formation in *Plasmopara viticola* , the causal agent of grapevine downy mildew, in highland regions of southern Brazil. Plant Pathology. 70:1897–1907.

Botero-Ramirez, A., Hwang, S.-F., and Strelkov, S. E. 2021. *Plasmodiophora brassicae* inoculum density and spatial patterns at the field level and relation to soil characteristics. Pathogens. 10:499.

Bourgade, E., Alonso Ugaglia, A., Bustillo, V., Dufourcq, T., Grimaldi, J., Guenser, J., et al. 2020. VITIFOREST□: Evaluation de l'impact de l'arbre agroforestier en contexte viticole. Innovations Agronomiques. 79:471–497.

Box, G. E. P., and Cox, D. R. 1964. An analysis of transformations. Journal of the Royal Statistical Society. 26:211–252.

Brischetto, C., Bove, F., Languasco, L., and Rossi, V. 2020. Can spore sampler data be used to predict *Plasmopara viticola* infection in vineyards? Front. Plant Sci. 11:1187.

Caffi, T., Rossi, V., and Lusitani, M. 2011. Long-term survival of *Plasmopara viticola* oospores. Integrated protection and production in viticulture IOBC/ wprs Bulletin. 67:111–114.

Campi, P., Palumbo, A. D., and Mastrorilli, M. 2009. Effects of tree windbreak on microclimate and wheat productivity in a Mediterranean environment. European Journal of Agronomy. 30:220–227.

Carisse, O. 2016. Development of grape downy mildew (*Plasmopara viticola*) under northern viticulture conditions: influence of fall disease incidence. Eur J Plant Pathol. 144:773–783.

Chatterton, S., Schwinghamer, T. D., Pagé, A., Davidson, R. B., Harding, M. W., and Banniza, S. 2023. Inoculum dose–disease response relationships for the pea root rot

pathogen, *Aphanomyces euteiches*, are dependent on soil type and other pathogens. Front. Plant Sci. 14:1115420.

Chen, W.-J., Delmotte, F., Cervera, S. R., Douence, L., Greif, C., and Corio-Costet, M.-F. 2007. At least two origins of fungicide resistance in grapevine downy mildew populations. Appl Environ Microbiol. 73:5162–5172.

Chiles, J.-P., and Delfiner, P. 1999. *Geostatistics: modeling spatial uncertainty*. New York: John Wiley & Sons.

Cressie, N. 1985. Fitting variogram models by weighted least squares. Mathematical Geology. 17:563–586.

Dagostin, S., Schärer, H.-J., Pertot, I., and Tamm, L. 2011. Are there alternatives to copper for controlling grapevine downy mildew in organic viticulture? Crop Protection. 30:776–788.

Dall'Agnol, J. C., Pezzini, M. F., Uribe, N. S., and Joveleviths, D. 2021. Systemic effects of the pesticide mancozeb – A literature review. European Review for Medical and Pharmacological Sciences. 25:4113–4120.

Delmas, C. E. L., Dussert, Y., Delière, L., Couture, C., Mazet, I. D., Richart Cervera, S., et al. 2017. Soft selective sweeps in fungicide resistance evolution: recurrent mutations without fitness costs in grapevine downy mildew. Molecular Ecology. 26:1936–1951.

Didelot, F., Caffier, V., Orain, G., Lemarquand, A., and Parisi, L. 2016. Sustainable management of scab control through the integration of apple resistant cultivars in a low-fungicide input system. Agriculture, Ecosystems & Environment. 217:41–48.

Douillet, A., Laurent, B., Beslay, J., Massot, M., Raynal, M., and Delmotte, F. 2022. LAMP for in-field quantitative assessments of airborne grapevine downy mildew inoculum. Journal of Applied Microbiology. 133:3404–3412.

Douillet, P. A. 2023. Étude pluriannuelle de la sporée aérienne de *Plasmopara viticola* par quantification moléculaire : un nouvel indicateur de risque des épidémies du mildiou de la vigne.

Favor, K., and Udawatta, R. P. 2021. Belowground services in vineyard agroforestry systems. In *Agroforestry and ecosystem services*, eds. Ranjith P. Udawatta and Jose Shibu. Springer International Publishing, p. 65–94.

Fontaine, M. C., Austerlitz, F., Giraud, T., Labbé, F., Papura, D., Richart-Cervera, S., et al. 2013. Genetic signature of a range expansion and leap-frog event after the recent invasion of Europe by the grapevine downy mildew pathogen *Plasmopara viticola*. Molecular Ecology. 22:2771–2786.

Fontaine, M. C., Labbé, F., Dussert, Y., Delière, L., Richart-Cervera, S., Giraud, T., et al. 2021. Europe as a bridgehead in the worldwide invasion history of grapevine downy mildew, *Plasmopara viticola*. Current Biology. 31:2155-2166.e4.

Gangneux, C., Cannesan, M.-A., Bressan, M., Castel, L., Moussart, A., Vicré-Gibouin, M., et al. 2014. A Sensitive Assay for Rapid Detection and Quantification of *Aphanomyces euteiches* in Soil. Phytopathology®. 104:1138–1147.

Gessler, C., Pertot, I., and Perazzolli, M. 2011. *Plasmopara viticola*: a review of knowledge on downy mildew of grapevine and effective disease management. Phytopathologia Mediterranea. 50:3–44.

Gobbin, D., Pertot, I., and Gessler, C. 2003. Identification of microsatellite markers for *Plasmopara viticola* and establishment of high throughput method for SSR analysis. European Journal of Plant Pahology. 109:153–164.

Gomez, C., Brun, L., Chauffour, D., and Vallée, D. D. L. 2007. Effect of leaf litter management on scab development in an organic apple orchard. Agriculture, Ecosystems & Environment. 118:249–255.

Goovaerts, P. 1998. Geostatistical tools for characterizing the spatial variability of microbiological and physico-chemical soil properties. Biology and Fertility of Soils. 27:315–334.

Gossen, B. D., Al-Daoud, F., Dumonceaux, T., Dalton, J. A., Peng, G., Pageau, D., et al. 2019. Comparison of techniques for estimation of resting spores of *Plasmodiophora brassicae* in soil. Plant Pathology. 68:954–961.

Goutouly, J., Drissi, R., Forget, D., and Gaudillère, J. 2006. Characterization of vine vigour by ground based NDVI measurements. VIth International Terroir Congress, Bordeaux, France. :237–241.

Grigera, M., Drijber, R., and Wienhold, B. 2007. Redistribution of crop residues during row cultivation creates a biologically enhanced environment for soil microorganisms. Soil and Tillage Research. 94:550–554.

Guérif, J., Richard, G., Dürr, C., Machet, J. M., Recous, S., and Roger-Estrade, J. 2001. A review of tillage effects on crop residue management, seedbed conditions and seedling establishment. Soil and Tillage Research. 61:13–32.

Hill, G. K. 1998. Studies on the germination of Plasmopara viticola oospores with a floating disc test.

Hong, C., Brewer, M. T., Brannen, P. M., and Scherm, H. 2020. Temporal disease dynamics and relative importance of sexual and asexual reproduction of grape downy mildew (*Plasmopara viticola*) in an isolated vineyard in the North Georgia Mountains, USA. Plant Pathology. 69:1721–1730.

Hugalde, I. P., Riaz, S., Agüero, C. B., Vila, H., Talquenca, S. G., and Walker, M. A. 2019. Studying growth and vigor as quantitative traits in grapevine populations. In *Integrated View of Population Genetics*, eds. RT Maia and MA Campos. London: IntechOpen, p. 9–24.

Hwang, S. F., Ahmed, H. U., Strelkov, S. E., Gossen, B. D., Turnbull, G. D., Peng, G., et al. 2011. Seedling age and inoculum density affect clubroot severity and seed yield in canola. Can. J. Plant Sci. 91:183–190.

Jacobs, S. R., Webber, H., Niether, W., Grahmann, K., Lüttschwager, D., Schwartz, C., et al. 2022. Modification of the microclimate and water balance through the integration of trees into temperate cropping systems. Agricultural and Forest Meteorology. 323:109065.

Jiang, G., Wang, N., Zhang, Y., Wang, Z., Zhang, Y., Yu, J., et al. 2021. The relative importance of soil moisture in predicting bacterial wilt disease occurrence. Soil Ecol. Lett. 3:356–366.

Journel, A. G., and Huijbregts, C. J. 1976. *Mining geostatistics*. London: Academic Press.

Kennelly, M. M., Gadoury, D. M., Wilcox, W. F., Magarey, P. A., and Seem, R. C. 2007. Primary infection, lesion productivity, and survival of sporangia in the grapevine downy mildew pathogen *Plasmopara viticola*. Phytopathology®. 97:512–522.

Lamichhane, J. R., Messéan, A., and Ricci, P. 2019. Chapter Two - Research and innovation priorities as defined by the Ecophyto plan to address current crop protection transformation challenges in France. In Advances in Agronomy, ed. Donald L. Sparks. Academic Press, p. 81–152. Available at: https://www.sciencedirect.com/science/article/pii/S0065211318300956.

Maddalena, G., Russo, G., and Toffolatti, S. L. 2021. The study of the germination dynamics of *Plasmopara viticola* oospores highlights the presence of phenotypic synchrony with the host. Front. Microbiol. 12:698586.

Matheron, G. 1963. Principles of geostatistics. Economic geology. 58:1246–1266.

Moussart, A., Wicker, E., Le Delliou, B., Abelard, J.-M., Esnault, R., Lemarchand, E., et al. 2009. Spatial distribution of *Aphanomyces euteiches* inoculum in a naturally infested pea field. Eur J Plant Pathol. 123:153–158.

Oliver, M. A., and Webster, R. 2014. A tutorial guide to geostatistics: Computing and modelling variograms and kriging. CATENA. 113:56–69.

Oliver, M. A., and Webster, R. 2015. *Basic steps in geostatistics: the variogram and kriging*. Cham: Springer International Publishing. Available at: https://link.springer.com/10.1007/978-3-319-15865-5 [Accessed February 21, 2024].

Pebesma, E. J. 2004. Multivariable geostatistics in S: the gstat package. Computers & Geosciences. 30:683–691.

Pennington, T. 2019. Natural pest suppression in vineyards under innovative management.

Peressotti, E., Wiedemann-Merdinoglu, S., Delmotte, F., Bellin, D., Di Gaspero, G., Testolin, R., et al. 2010. Breakdown of resistance to grapevine downy mildew upon limited deployment of a resistant variety. BMC Plant Biol. 10:147.

Pertot, I., and Zulini, L. 2003. Studies on *Plasmopara viticola* oospore germination in Trentino, Italy. IOBC WPRS Bulletin. 26:43–46.

R Core Team. 2023. R: A language and environment for statistical computing. Available at: https://www.R-project.org/.

Rački, N., Dreo, T., Gutierrez-Aguirre, I., Blejec, A., and Ravnikar, M. 2014. Reverse transcriptase droplet digital PCR shows high resilience to PCR inhibitors from plant, soil and water samples. Plant Methods. 10:42.

Rouxel, M., Mestre, P., Comont, G., Lehman, B. L., Schilder, A., and Delmotte, F. 2013. Phylogenetic and experimental evidence for host-specialized cryptic species in a biotrophic oomycete. New Phytologist. 197:251–263.

Schneider, O., Roger-Estrade, J., Aubertot, J.-N., and Doré, T. 2006. Effect of seeders and tillage equipment on vertical distribution of oilseed rape stubble. Soil and Tillage Research. 85:115–122.

Si Ammour, M., Bove, F., Toffolatti, S. L., and Rossi, V. 2020. A Real-Time PCR assay for the quantification of *Plasmopara viticola* oospores in grapevine leaves. Front. Plant Sci. 11:1202.

Valsesia, G., Gobbin, D., Patocchi, A., Vecchione, A., Pertot, I., and Gessler, C. 2005. Development of a high-throughput method for quantification of *Plasmopara viticola* DNA in grapevine leaves by means of quantitative real-time polymerase chain reaction. Phytopathology®. 95:672–678.

Vercesi, A., Toffolatti, S. L., Zocchi, G., Guglielmann, R., and Ironi, L. 2010. A new approach to modelling the dynamics of oospore germination in *Plasmopara viticola*. Eur J Plant Pathol. 128:113–126.

Vercesi, A., Tornaghi, R., Sant, S., Burruano, S., and Faoro, F. 1999. A cytological and ultrastructural study on the maturation and germination of oospores of *Plasmopara viticola* from overwintering vine leaves. Mycological Research. 103:193–202.

Weerakoon, N. D., Roberts, J. K., Lehnen, L. P., Wilkinson, J. M., Marshall, J. S., and Hardham, A. R. 1998. Isolation and characterization of the single β-tubulin gene in *Phytophthora cinnamomi*. Mycologia. 90:85–95.

Wen, R., Lee, J., Chu, M., Tonu, N., Dumonceaux, T., Gossen, B. D., et al. 2020. Quantification of *Plasmodiophora brassicae* resting spores in soils using droplet digital PCR (ddPCR). Plant Disease. 104:1188–1194.

Weninger, T., Scheper, S., Lackóová, L., Kitzler, B., Gartner, K., King, N. W., et al. 2021. Ecosystem services of tree windbreaks in rural landscapes—a systematic review. Environ. Res. Lett. 16:103002.

Wickham, H. 2016. *ggplot2: Elegant graphics for data analysis*. New York: Springer-Verlag.

Wong, F. P., Burr, H. N., and Wilcox, W. F. 2001. Heterothallism in *Plasmopara viticola*. Plant Pathology. 50:427–432.

Zhang, C., Selinus, O., and Schedin, J. 1998. Statistical analyses for heavy metal contents in till and root samples in an area of southeastern Sweden. The Science of The Total Environment. 212:217–232.

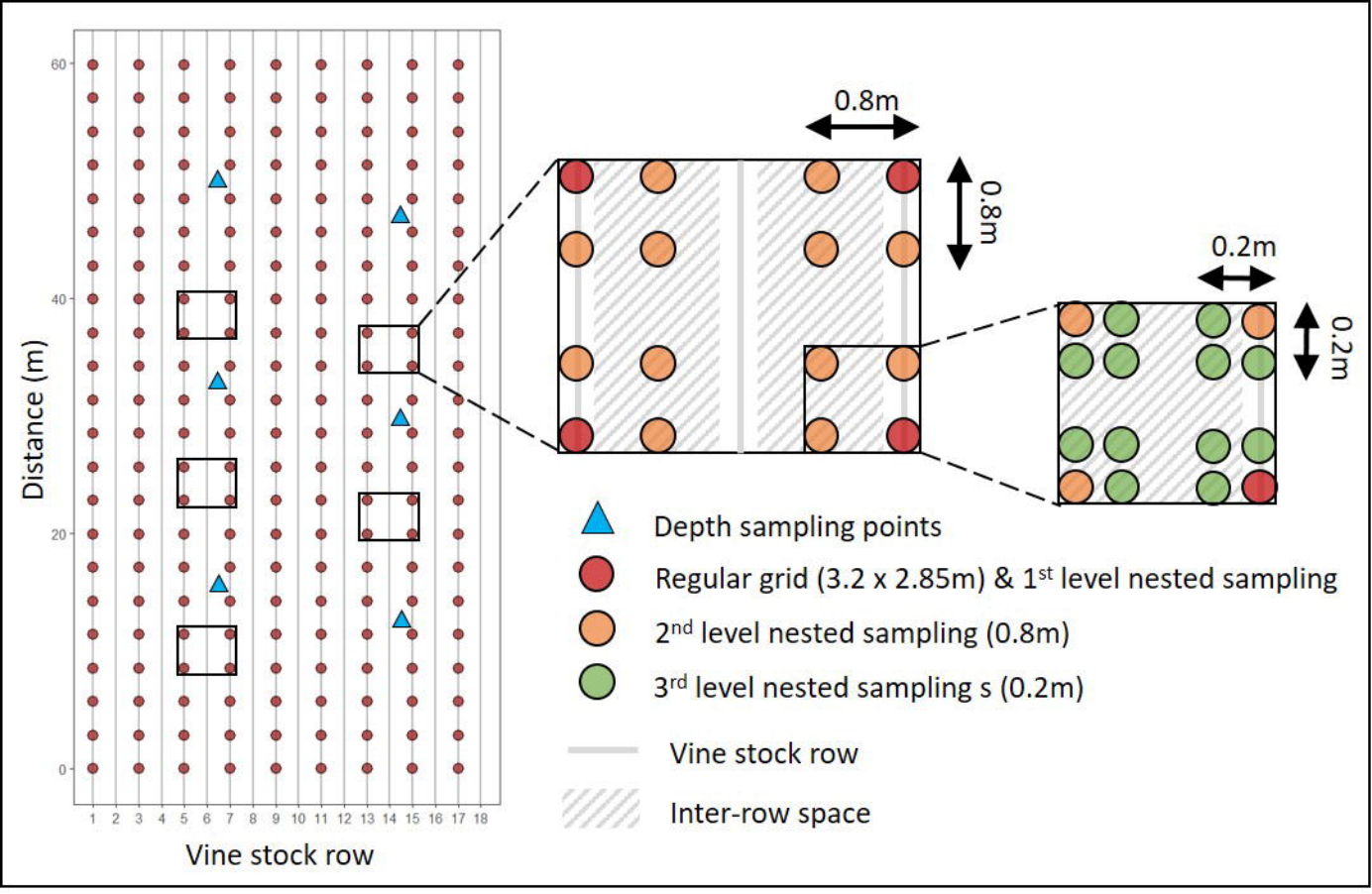
Distance (m)
60
40
20
0
1 2 3 4 5 6 7 8 9 10 11 12 13 14 15 16 17 18
Vine stock row
0.8m
0.8m
0.2m
0.2m
Depth sampling points
Regular grid (3.2 x 2.85m) & 1st level nested sampling
2nd level nested sampling (0.8m)
3rd level nested sampling s (0.2m)
Vine stock row
Inter-row space

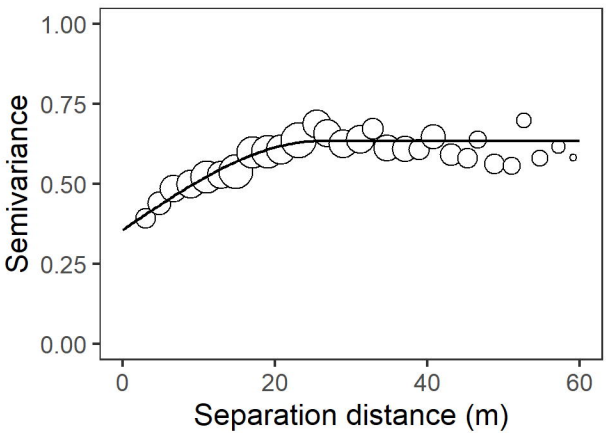
Semivariance
1.00
0.75
0.50
0.25
0.00
0
20
40
60
Separation distance (m)

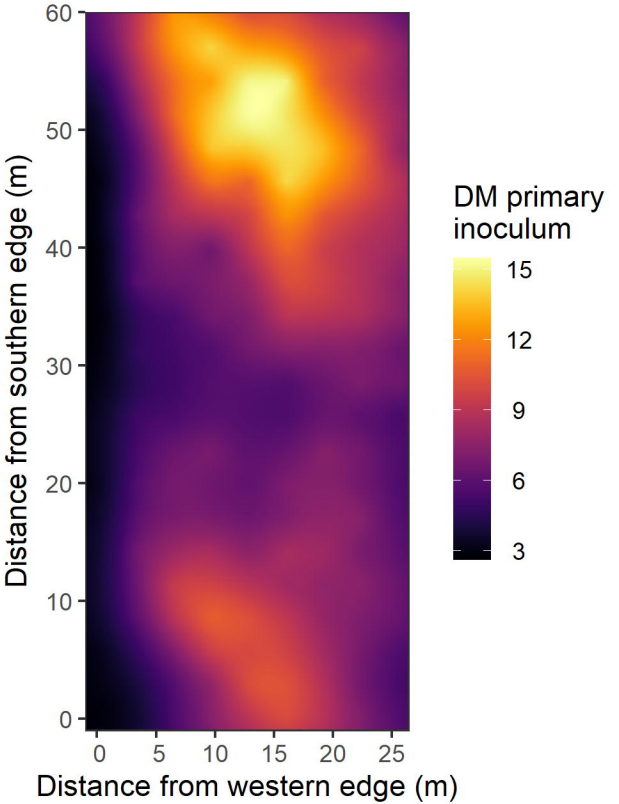
Distance from southern edge (m)
60
50
40
30
20
10
0
0
5
10
15
20
25
Distance from western edge (m)
DM primary inoculum
15
12
9
6
3

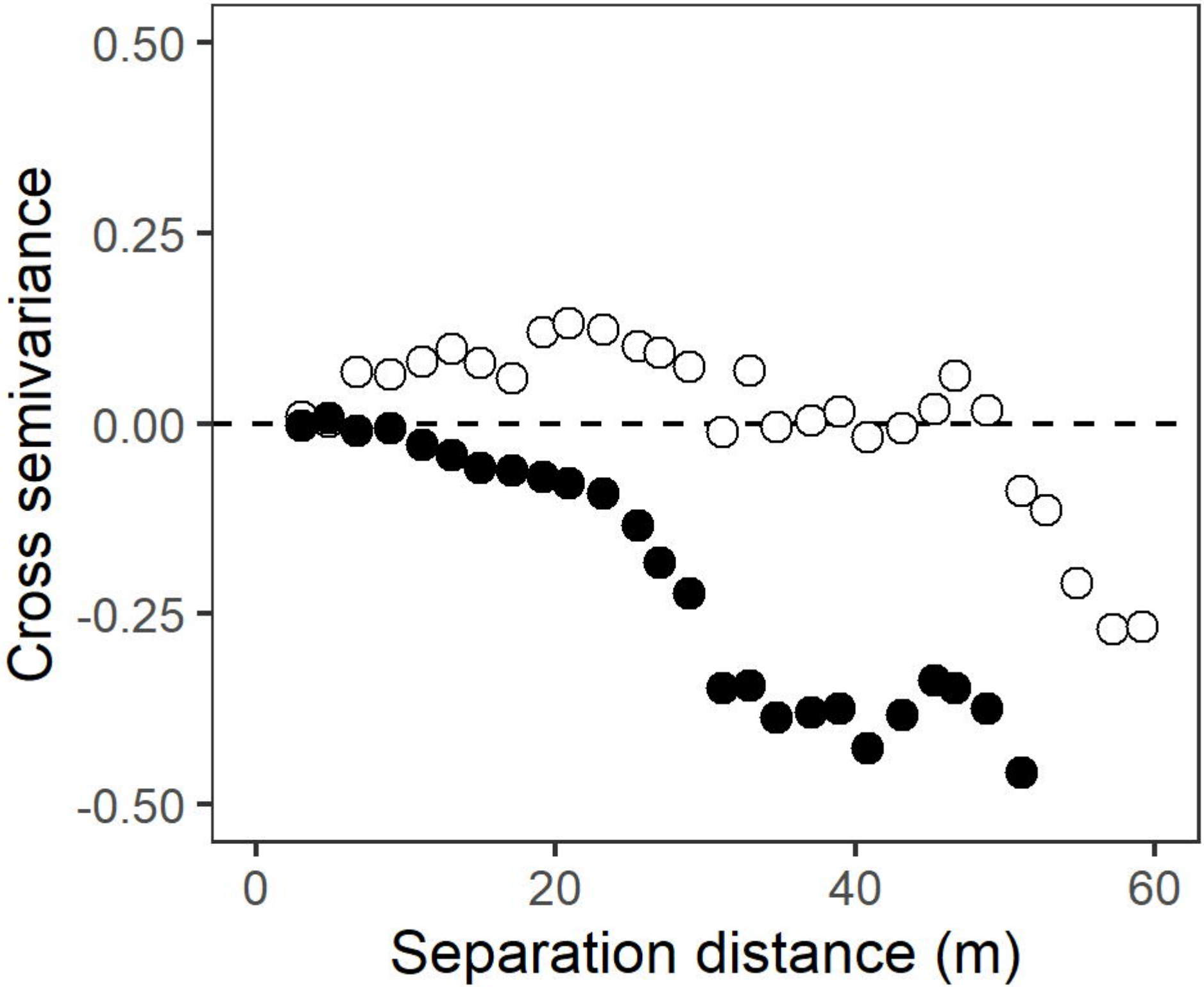
0.50
0.25
0.00
-0.25
-0.50
Cross semivariance
0
20
40
60
Separation distance (m)

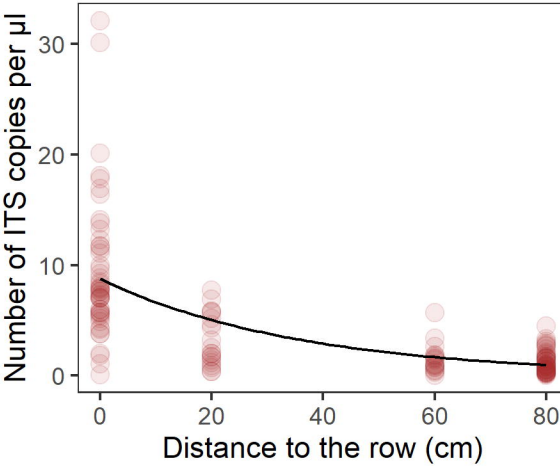
Number of ITS copies per µl
30
20
10
0
0
20
40
60
80
Distance to the row (cm)

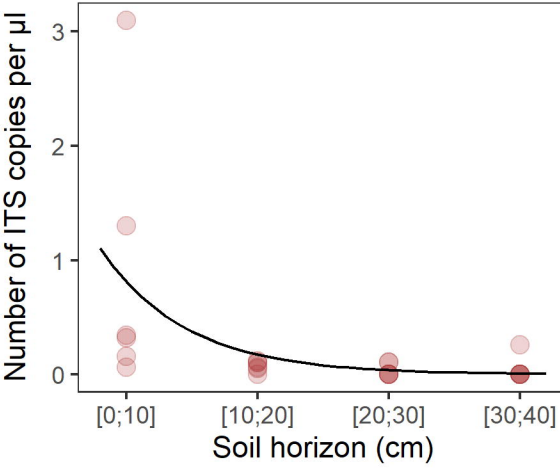
Number of ITS copies per µl
3
2
1
0
[0;10]
[10;20]
[20;30]
[30;40]
Soil horizon (cm)

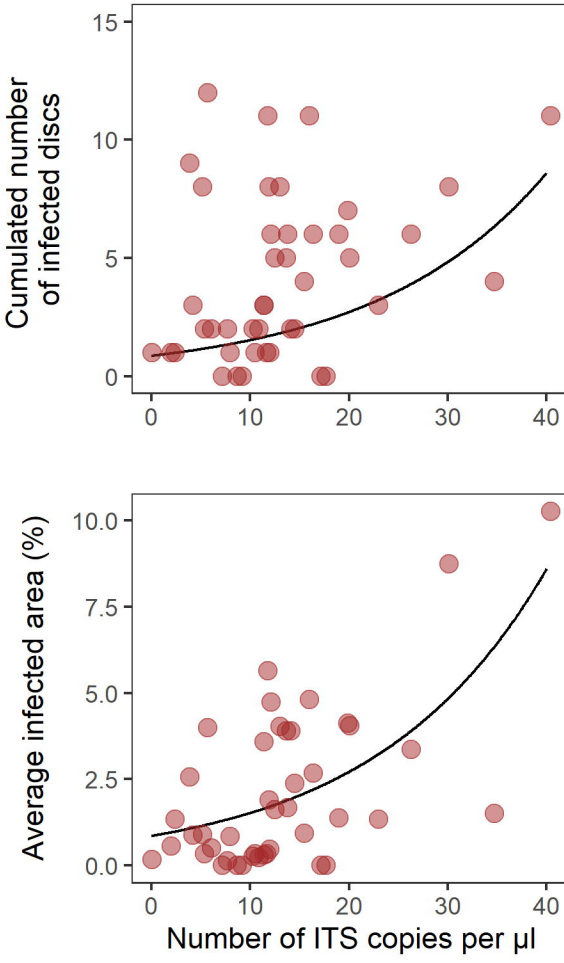
Cumulated number of infected discs
15
10
5
0
0
10
20
30
40
Average infected area (%)
10.0
7.5
5.0
2.5
0.0
0
10
20
30
40
Number of ITS copies per µl

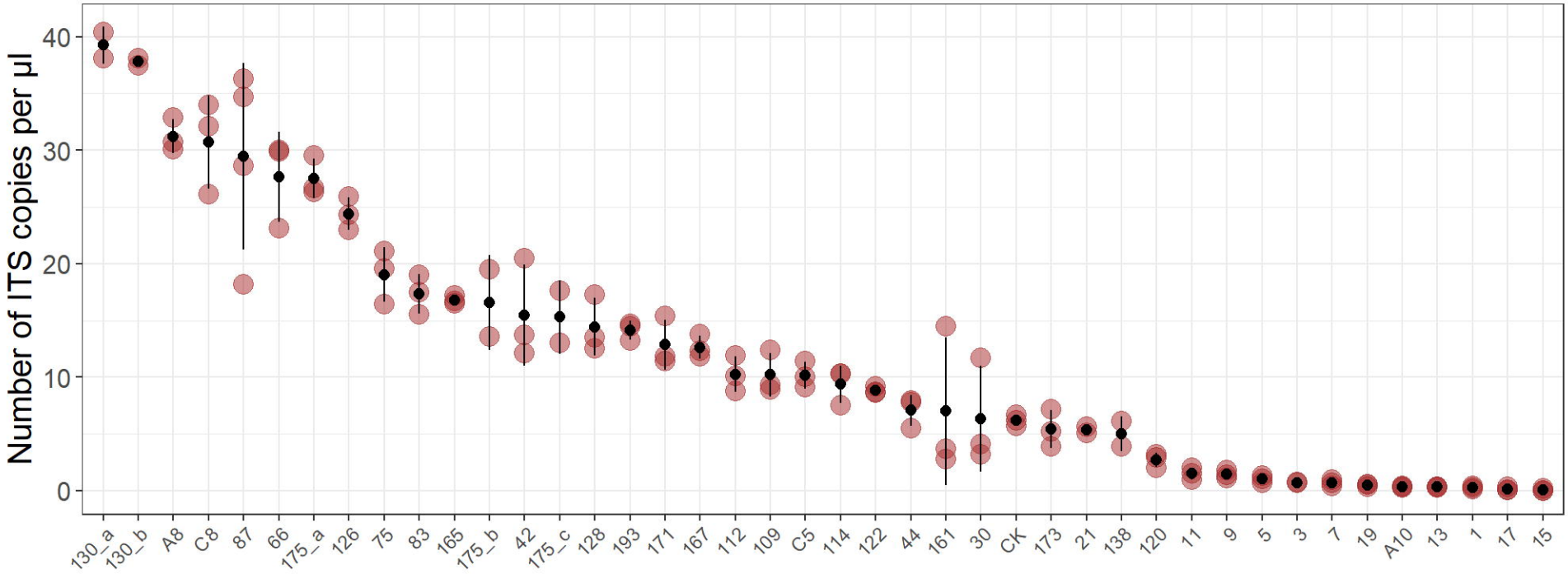
Number of ITS copies per µl
40
30
20
10
0
130_a
130_b
A8
C8
87
66
175_a
126
75
83
165
175_b
42
175_c
128
193
171
167
112
109
C5
114
122
44
161
30
CK
173
21
138
120
11
9
5
3
7
19
A10
13
1
17
15

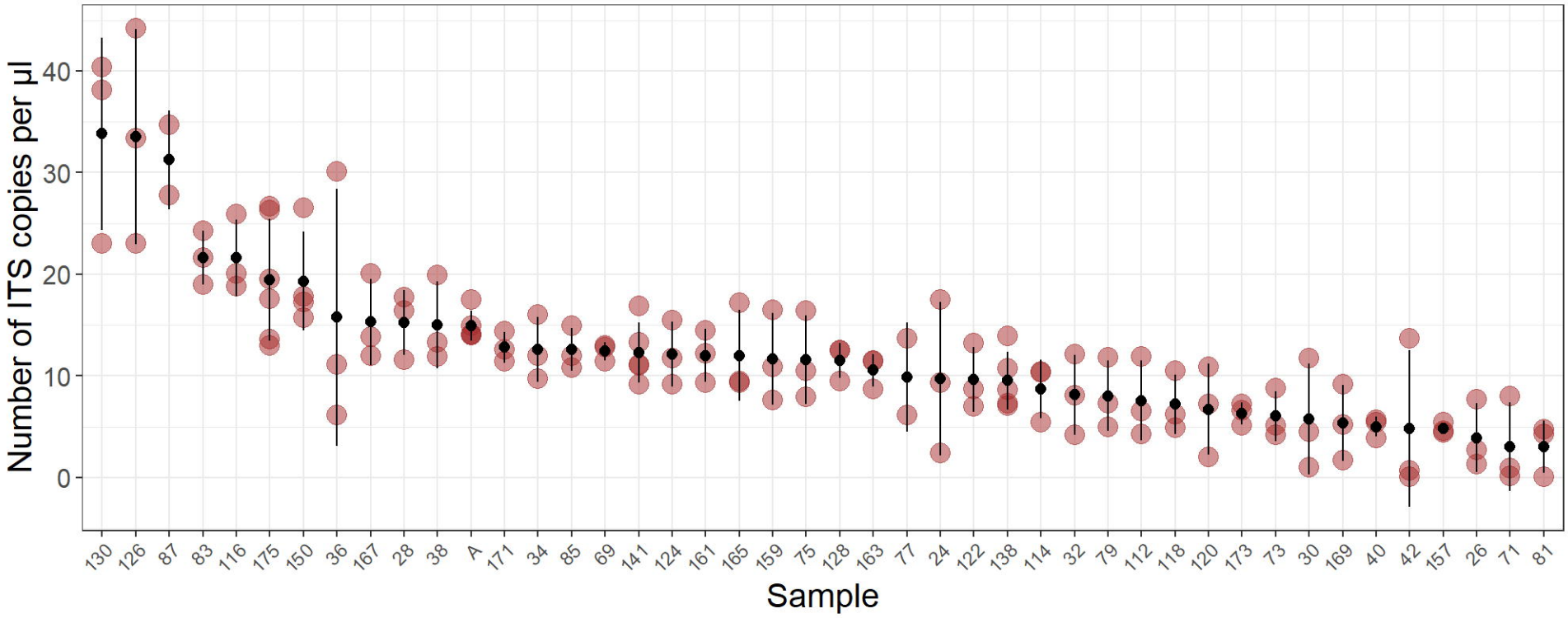
Number of ITS copies per µl
40
30
20
10
0
130
126
87
83
116
175
150
36
167
28
38
A
171
34
85
69
141
124
161
165
159
75
128
163
77
24
122
138
114
32
79
112
118
120
173
73
30
169
40
42
157
26
71
81
Sample